

Supporting Information

## Excellent Photoreduction Performance of Cr(VI) over $(\text{WO}_4)^{2-}$ -Doped Metal Organic Framework Materials

Xinyun Zhao<sup>1\*</sup>, Lamei Wu<sup>1</sup>, Xi Chen<sup>1</sup>, Juncheng Hu<sup>1</sup>, Tsung-hsueh Wu<sup>2</sup>, Qin Li<sup>1</sup>,  
Kangle Lv<sup>1</sup>

<sup>1</sup> Hubei Key Laboratory of Catalysis and Materials Science, School of Chemistry and Materials Science, South-Central University for Nationalities, Wuhan 430074, China

<sup>2</sup>Department of Chemistry, University of Wisconsin-Platteville, Platteville, 53818, USA

1. Fig.S1: Enlarged power XRD patterns of different samples with  $2\theta$  from  $5^\circ$  to  $10^\circ$
2. Fig.S2: XPS patterns of C1s within  $0.4\text{Na}_2\text{WO}_4$  BiBDC
3. Fig.S3a-3e: Raman spectra of as-prepared samples
4. Fig.S4a-4e: FT-IR spectra of as-prepared samples
5. Fig.S5: DRS of as-samples
6. Fig.S6. SEM images of as-prepared samples
7. Fig.S7. Recycling and stability of catalyst

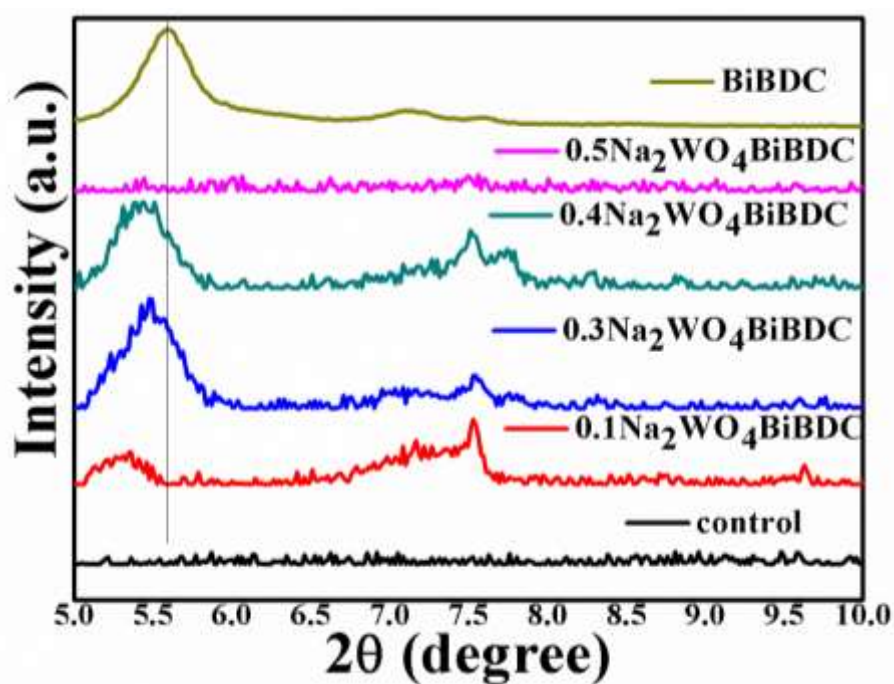


Fig.S1: Enlarged power XRD patterns of different samples with  $2\theta$  from 5 to  $10^\circ$

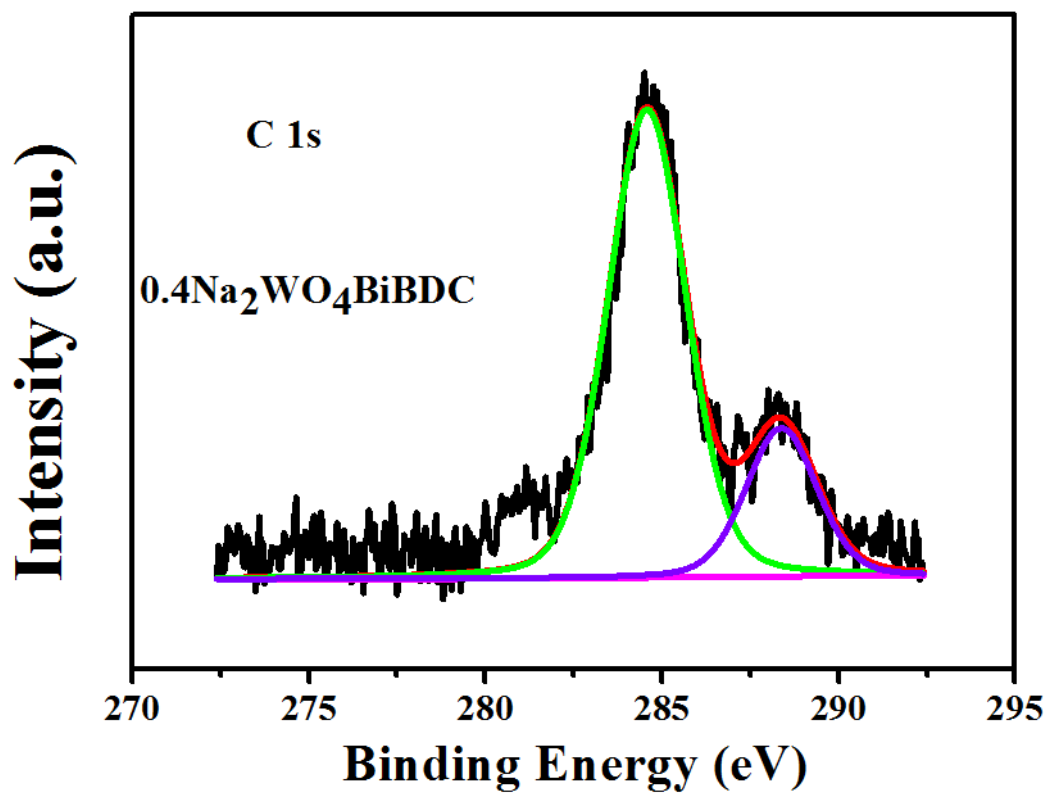


Fig.S2: XPS patterns of C1s within 0.4Na<sub>2</sub>WO<sub>4</sub> BiBDC

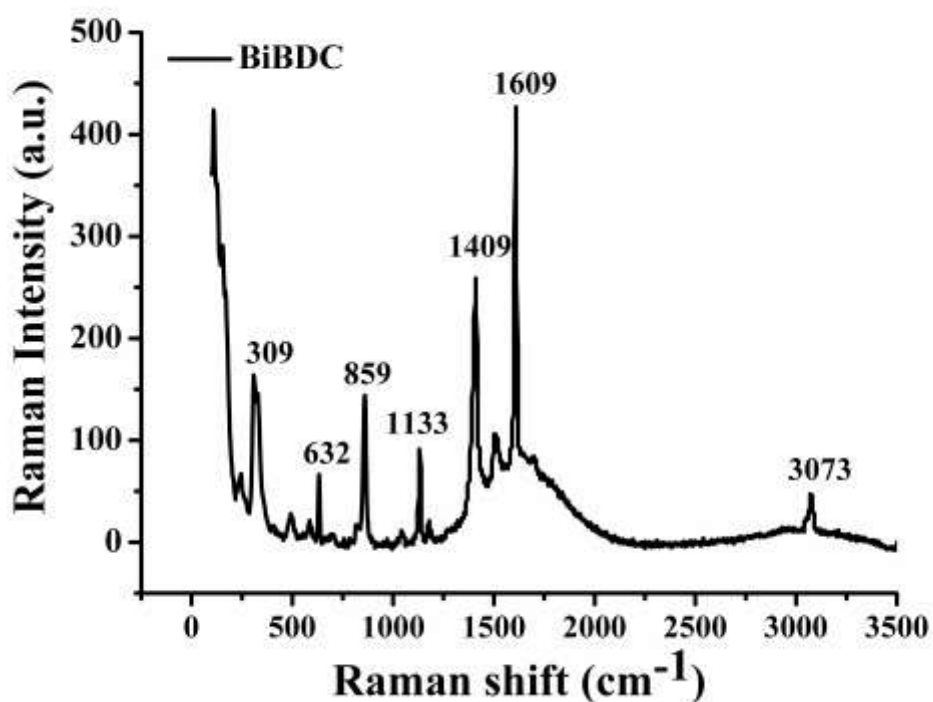


Fig.S3a. Raman spectra of BiBDC

Bismuth terephthalate shows characteristic Raman vibrational peaks at 1609(s), 1505 (w), 1409(s), 1133(w), 859(s), 632(w) and 309(s)  $\text{cm}^{-1}$ . The bands at 3073  $\text{cm}^{-1}$  and 1609  $\text{cm}^{-1}$  are ascribed to  $\nu_{(\text{C-H})}$  and  $\nu_{(\text{C=C})}$  modes of the benzene ring. While the peaks at 1505 and 1409  $\text{cm}^{-1}$  are ascribed to the asymmetric and symmetric stretch modes of the coordinated  $-\text{COO}^-$  groups. The peak at 1133  $\text{cm}^{-1}$  is attributed to terephthalate ring breathing and benzoate ring deformation. The peaks at 859 and 632  $\text{cm}^{-1}$  are associated with the deformation modes of C–H out of phase and benzene ring deformation in terephthalates. The peak at 309  $\text{cm}^{-1}$  of bismuth terephthalate is important to monitor as it can be attributed to the presence of vibrational modes involving  $\text{Bi}^{3+}$  species.

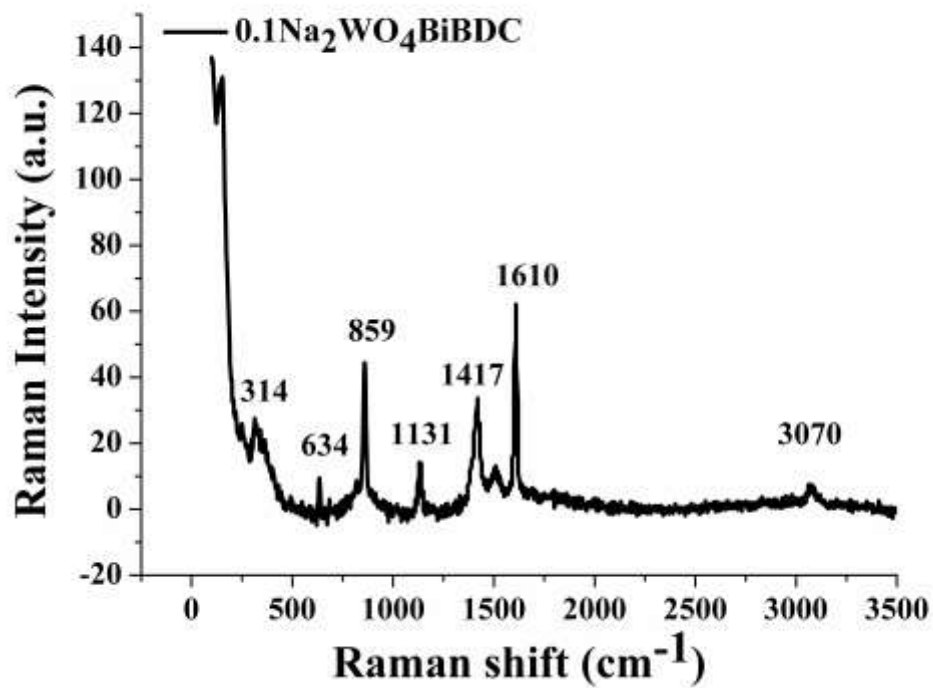


Fig.S3b. Raman spectra of 0.1Na<sub>2</sub>WO<sub>4</sub>BiBDC

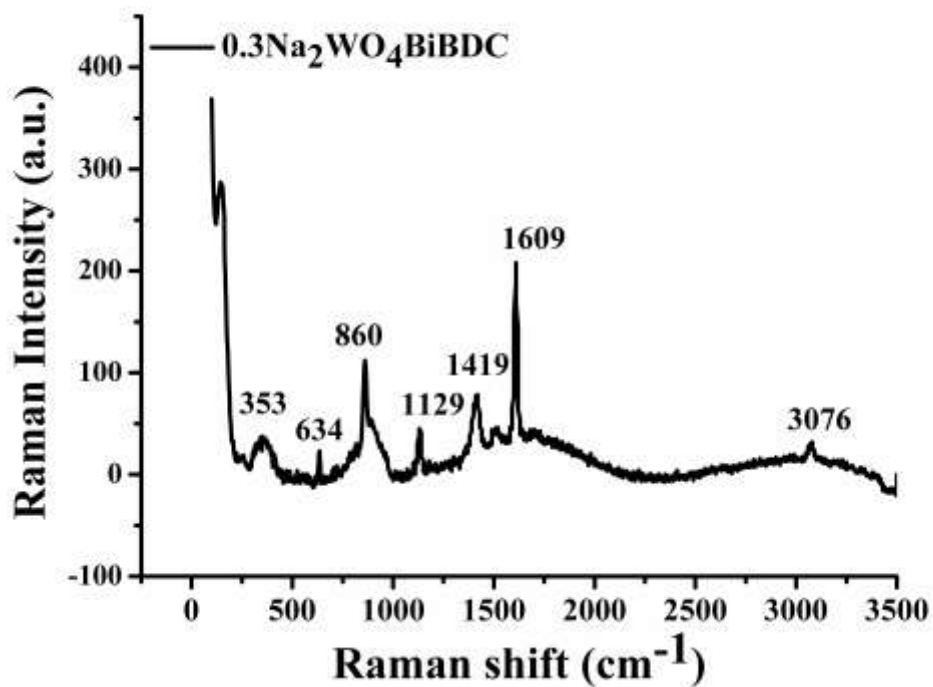


Fig.S3c. Raman spectra of 0.3Na<sub>2</sub>WO<sub>4</sub>BiBDC

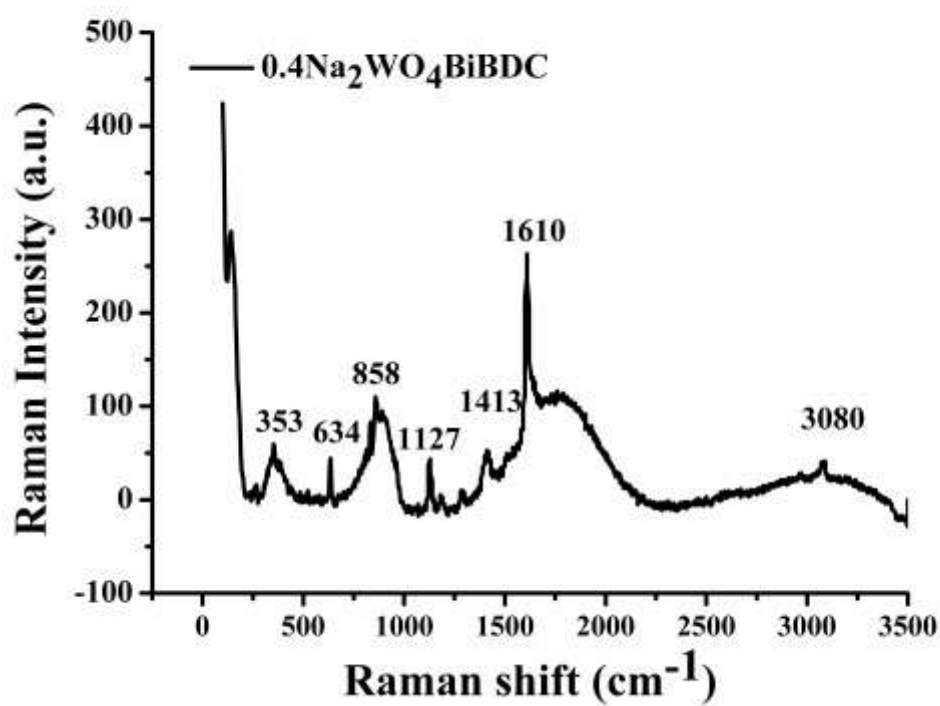


Fig.S3d. Raman spectra of 0.4Na<sub>2</sub>WO<sub>4</sub>BiBDC

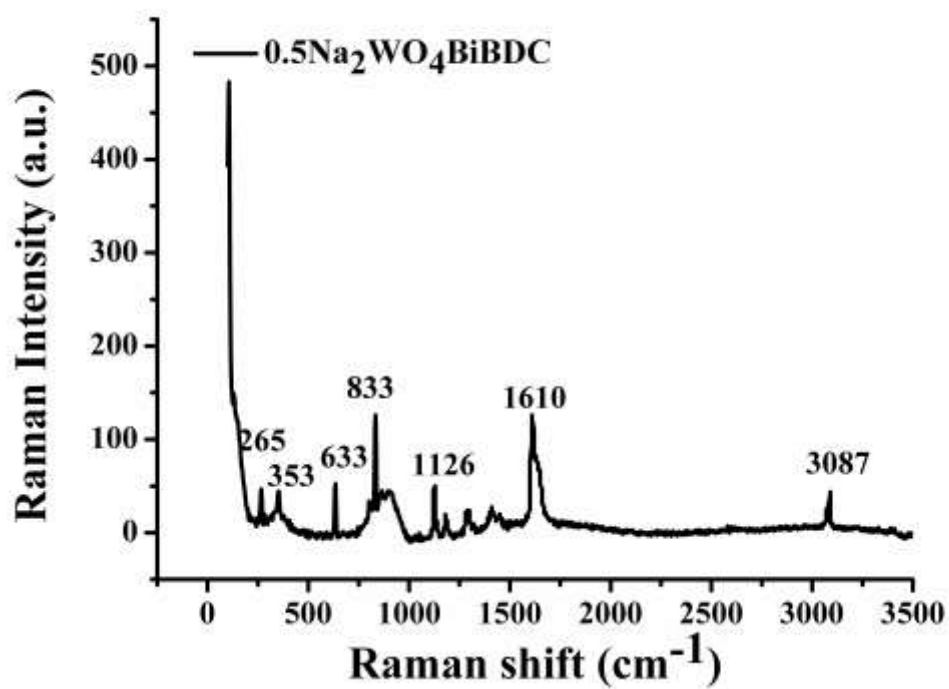


Fig.S3e. Raman spectra of 0.5Na<sub>2</sub>WO<sub>4</sub>BiBDC

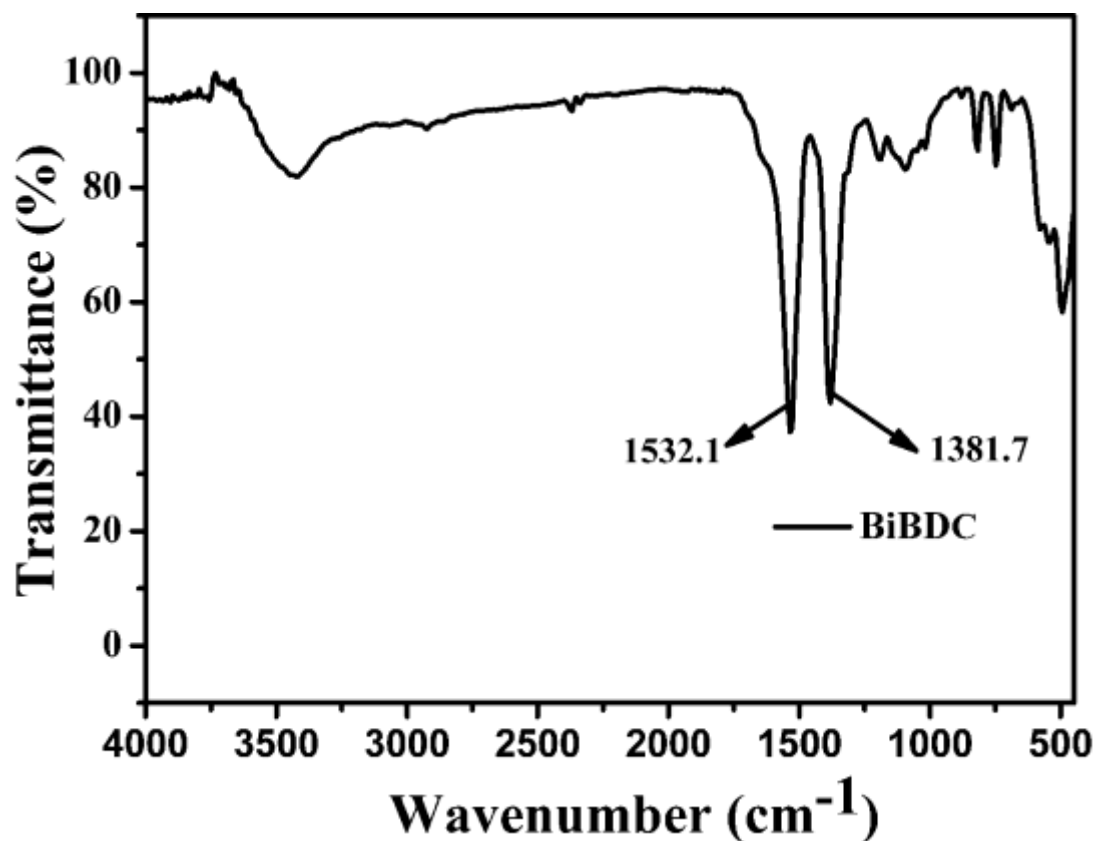


Fig.S4a. FT-IR spectra of BiBDC

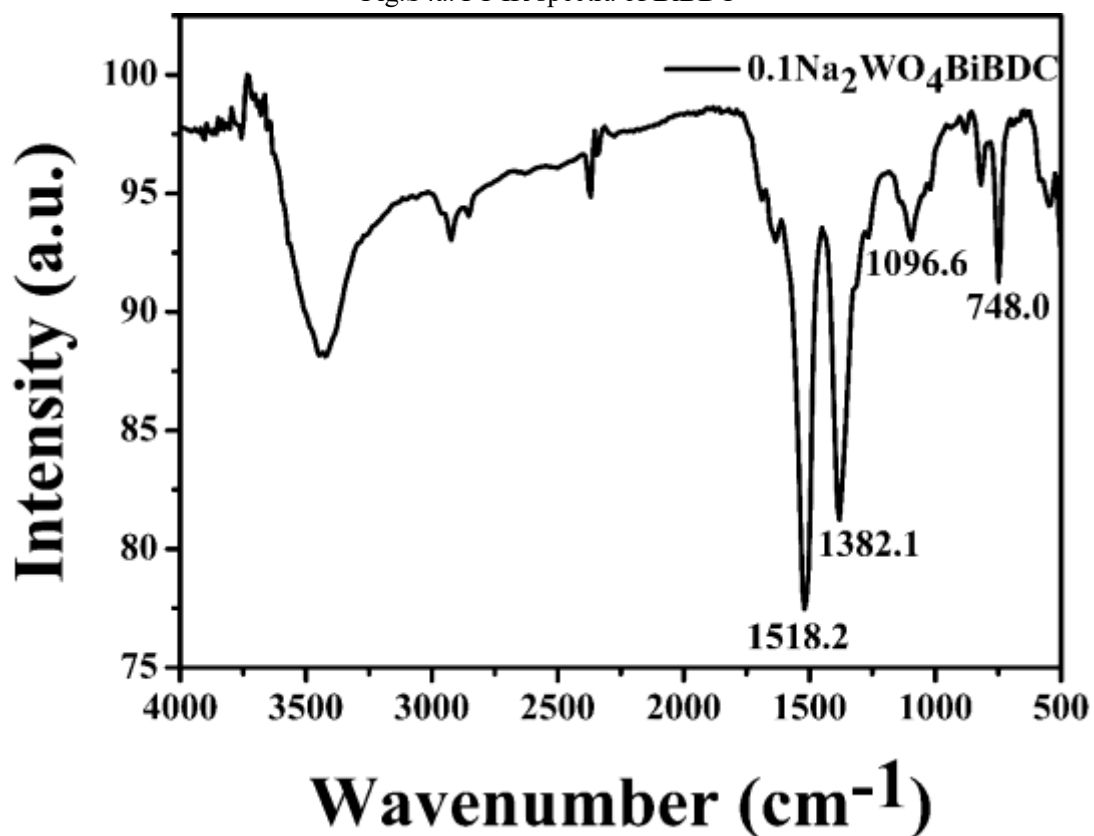


Fig.S4b. FT-IR spectra of 0.1Na<sub>2</sub>WO<sub>4</sub>BiBDC

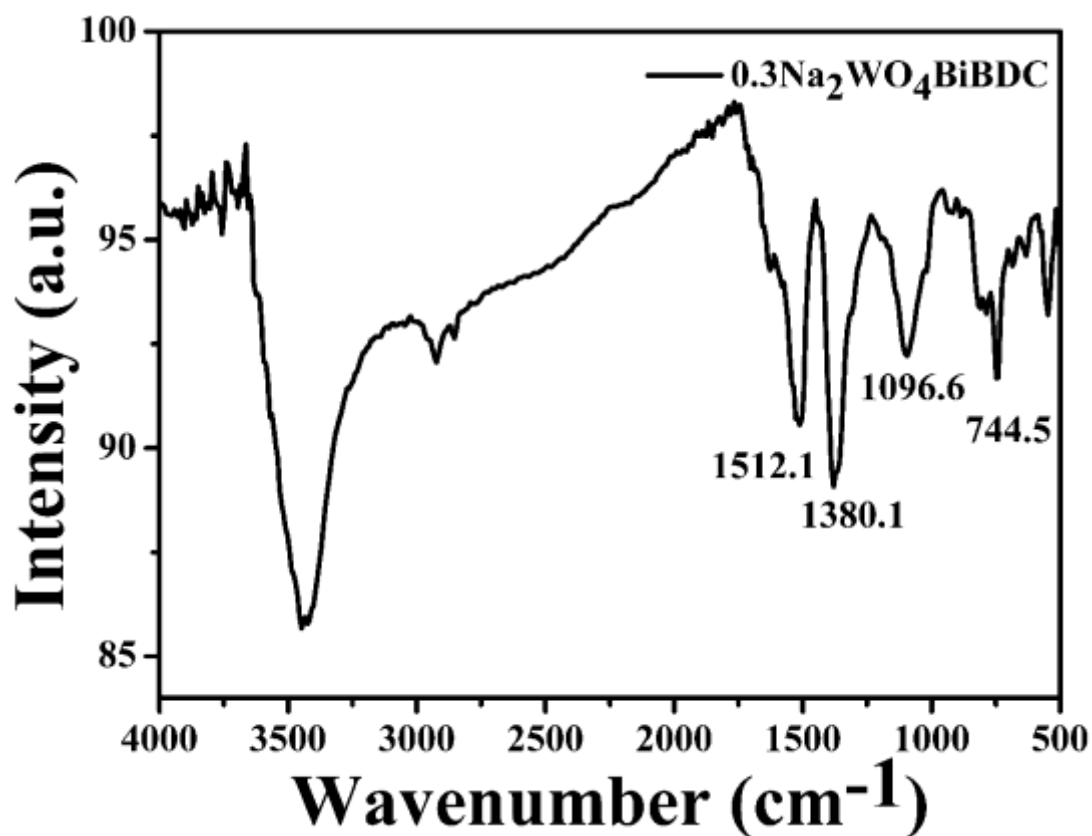


Fig.S4c. FT-IR spectra of 0.3Na<sub>2</sub>WO<sub>4</sub>BiBDC

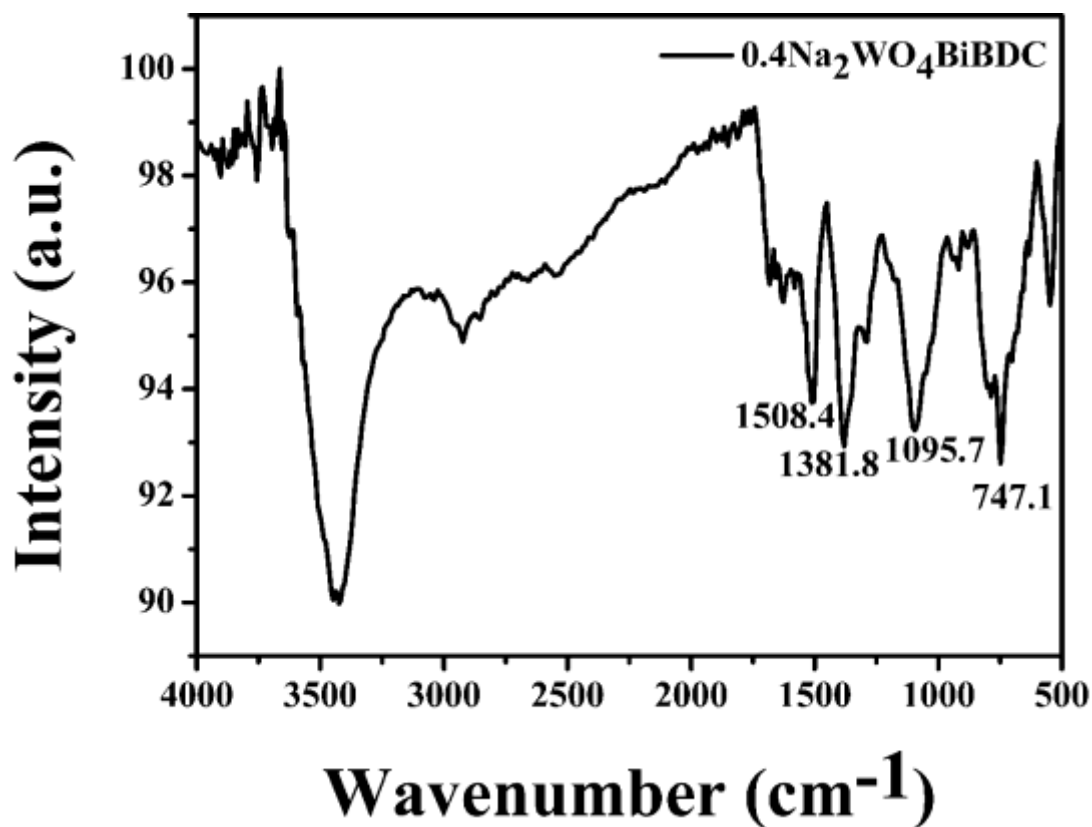


Fig.S4d. FT-IR spectra of 0.4Na<sub>2</sub>WO<sub>4</sub>BiBDC

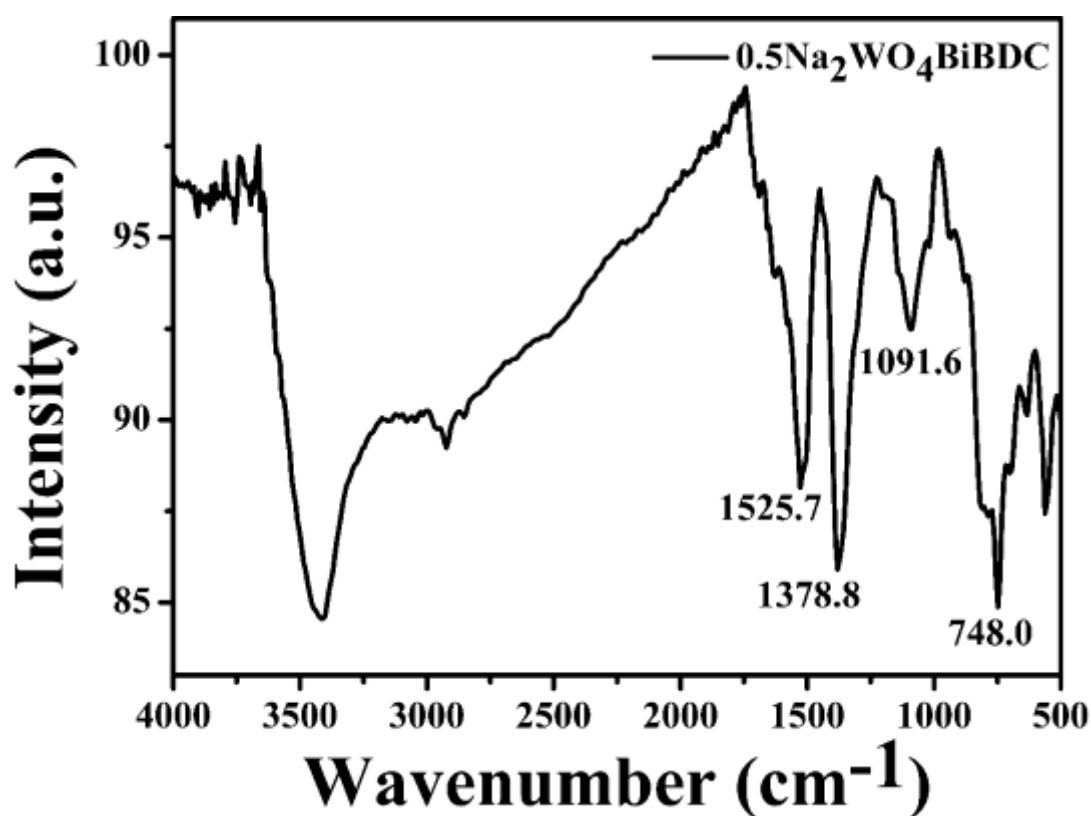


Fig.S4e. FT-IR spectra of 0.5Na<sub>2</sub>WO<sub>4</sub>BiBDC

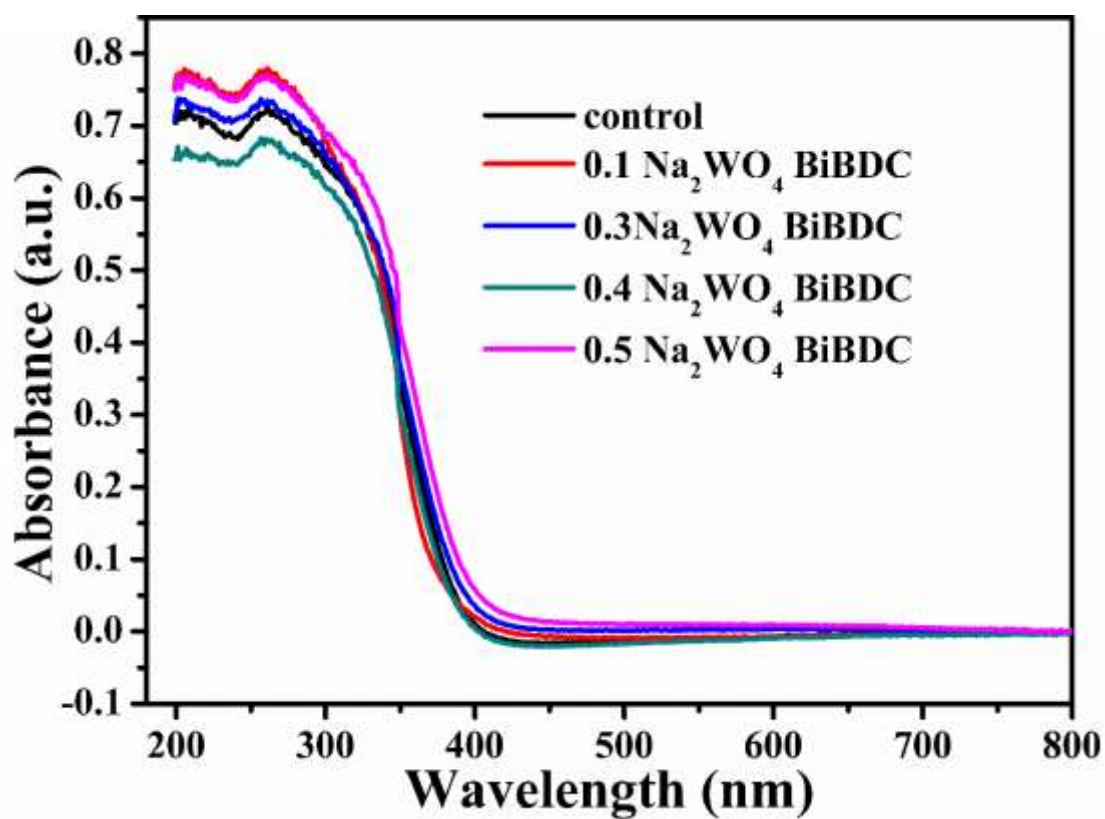


Fig.S5. DRS of as-prepared samples

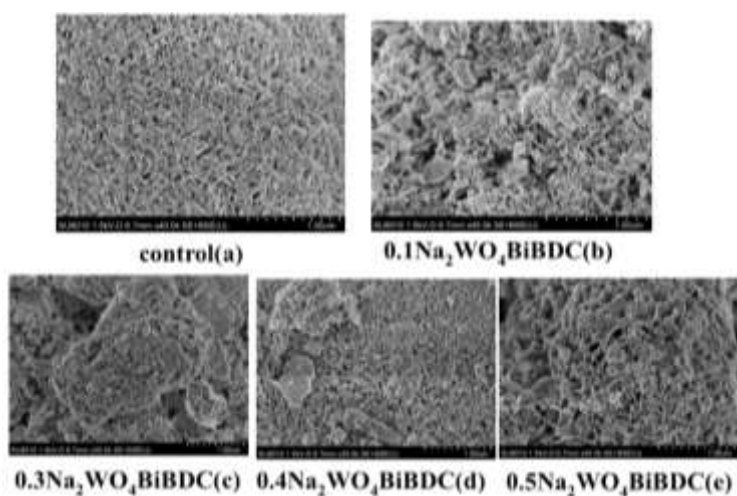


Fig.S6. SEM images of as-prepared samples

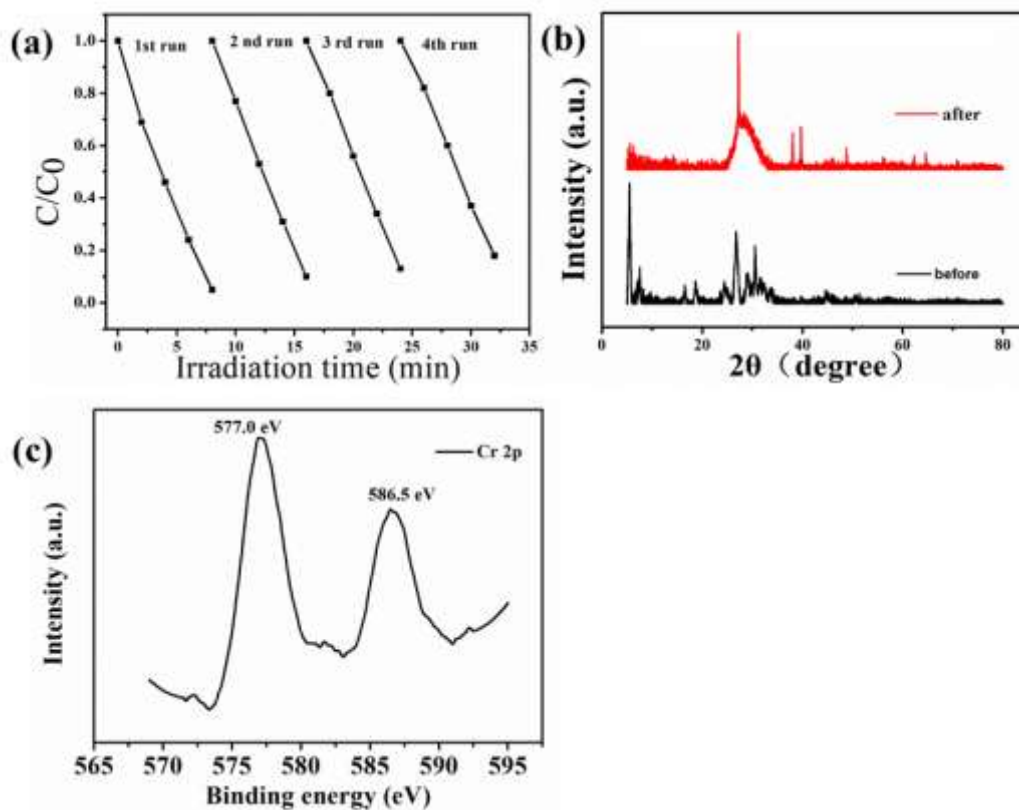


Fig.S7. Recycling and stability of the catalyst. C/C<sub>0</sub> of Cr(VI) with irradiation time plot (a) and XRD patterns of 0.3Na<sub>2</sub>WO<sub>4</sub>BiBDC before and after using (b), XPS analysis of Cr after 4<sup>th</sup> recycling use over 0.3Na<sub>2</sub>WO<sub>4</sub>BiBDC (c)